Michael R. Hill,[1] R. Doug Carpenter,[1] Glaucio H. Paulino,[2] Zuhair A. Munir,[1] and Jeffery C. Gibeling[1]

# Fracture Testing of a Layered Functionally Graded Material

**Reference:** Hill, M. R., Carpenter, R. D., Paulino, G. H., Munir, Z. A., and Gibeling, J. C., **"Fracture Testing of a Layered Functionally Graded Material,"** *Fracture Resistance Testing of Monolithic and Composite Brittle Materials, ASTM STP 1409*, J. A. Salem, G. D. Quinn, and M. G. Jenkins, Eds., American Society for Testing and Materials, West Conshohocken, PA, 2002.

**Abstract:** This paper describes measurements of the $K_I$ R-curve for a layered ceramic-metallic functionally graded material (FGM) composed of Ti and TiB phases. Single edge notch bend specimens were fabricated for crack propagation perpendicular to the graded layers from the brittle to the ductile side of the FGM. The precracking method and residual stresses affected the measured toughness. A new reverse bending method produced a sharp precrack without damaging the material. A representative sample indicates R-curve behavior rising from $K_{meas}$ = 7 MPa·m$^{1/2}$ in the initial crack-tip location (38% Ti and 62% TiB) to 31 MPa·m$^{1/2}$ in pure Ti. Residual stresses acting normal to the crack-plane were measured in the parent plate using the crack compliance technique. The residual stress intensity factor in the SE(B) specimen determined from the weight function was -2.4 MPa·m$^{1/2}$ at the initial precrack length. Thus, the actual material toughness at the start of the test was 34% less than the measured value.

**Keywords:** Functionally graded material, residual stress, fracture toughness, R-curve

## Introduction

A functionally graded material (FGM) is a composite containing at least two distinct phases that vary in relative proportions along at least one dimension of the solid. The classic example is that of a metallic/ceramic FGM that is predominantly metallic on one side of a plate and continuously becomes more ceramic through the thickness. The primary goal in designing such materials is to take advantage of the desirable properties

[1] Assistant Professor, Department of Mechanical and Aeronautical Engineering; Graduate student, Professor and Professor, respectively, Department of Chemical Engineering and Materials Science, University of California, One Shields Avenue, Davis, CA 95616.

[2] Assistant Professor, Department of Civil and Environmental Engineering, University of Illinois, Urbana IL 61801-2352.

of the ceramic, such as high hardness, corrosion resistance, and high melting temperature, while retaining the benefits of the metallic phase including good fracture toughness, machinability, and weldability. When discrete layers of metal and ceramic are used, the difference in coefficients of thermal expansion can lead to high internal stresses. Thus, another advantage of a graded composition lies in avoiding problems associated with high thermal and residual stresses. To achieve these design goals, it is necessary to understand and control the variation in properties and the gradient in composition.

FGMs have been produced by a variety of methods, including chemical vapor deposition [*1*], powdered metal sintering [*2*], high-temperature plasma spraying [*3*], self-propagating combustion synthesis (SHS) [*4*, *5*], thermo-chemical diffusion, and sedimentation of slurried powders [*6*]. As a practical matter, synthesis of materials with a continuous variation in the relative volume fractions of the two constituents may be difficult. Thus, numerous investigators have created discontinuous or layered FGMs. When the material is cooled from the synthesis temperature, residual stresses generally develop at the interfaces between layers. Although the residual stresses can be minimized by varying the composition in smaller steps, their presence can nonetheless limit the utility of a FGM.

As noted above, one motivation for developing functionally graded materials is to avoid problems associated with the low toughness of many ceramics. Thus, fracture toughness is a limiting property in the development of FGMs. For that reason, a number of authors have presented mathematical treatments of the fracture resistance of functionally graded materials [*7*-*9*]. These studies have shown that the crack tip fields for general non-homogeneous materials are identical to those in a homogenous material provided the properties of the former are continuous and piece-wise continuously differentiable [*8*]. Under these conditions it is possible to extend the concept of the stress intensity factor to study fracture and fracture toughness of FGMs. Jin and Batra [*9*, *10*] have presented a theoretical prediction of rising R-curve behavior in a metallic/ceramic FGM based on specimen size, loading conditions, and metal particle size. They used a simple linear rule of mixtures for Young's modulus, shear modulus, and Poisson's ratios and noted that “the micro-mechanical models developed for macro-homogeneous composites are only approximately valid for FGMs.”

In contrast, there is a relative scarcity of experimental fracture studies on FGMs due primarily to the lack of materials of size sufficient to produce standard fracture testing specimens. However, recent advances in processing methods have resulted in the production of larger FGMs. For the present study, we acquired a Ti/TiB FGM with dimensions 150mm x 150mm and 16mm thick from Cercom, Inc. The dimensions of this plate are sufficient to permit single edge notch beams to be machined for standard fracture experiments.

Thus, the goal of the present paper is to provide experimental measurements of the fracture toughness of functionally graded materials and to extend the concepts embodied in fracture mechanics testing standards to this new class of materials. We address problems associated with precracking, crack length measurement, and data reduction. We demonstrate that rising R-curve behavior is observed in a layered Ti/TiB FGM when the crack propagates from the more brittle side to the more ductile composition. In addition, we quantitatively account for residual stresses and show that they can have a significant effect on the measured fracture toughness values.

## Material and Experimental Procedure

### *Material*

The material tested in this study was a layered, functionally graded titanium/titanium monoboride plate. This material was prepared by Cercom, Inc. using a commercially pure titanium metal base. Tape cast layers composed of various mixtures of titanium and titanium diboride powders were placed on top of this plate. The assembled laminate was hot pressed at 1578K at a pressure of 13.8 MPa. In order to facilitate densification at this temperature, a proprietary sintering aid containing nickel was added to the starting powders. This material created a liquid phase at 1215K that also catalyzed the reaction of titanium and $TiB_2$ to form TiB with virtually no residual $TiB_2$. The resulting FGM was composed of seven layers ranging from pure Ti on one side to 85 volume% TiB on the other. The compositions of each of the layers of this FGM are listed in Table 1.

*Table 1 – Composition and elastic properties of the Ti/TiB FGM*

| Layer # | vol% Ti | vol% TiB | d (mm)* | E (GPa) | $\nu$ |
|---|---|---|---|---|---|
| 1 | 15 | 85 | 2.5 | 312.67 | 0.14 |
| 2 | 21 | 79 | 1.7 | 303.37 | 0.152 |
| 3 | 38 | 62 | 1.8 | 289.38 | - |
| 4 | 53 | 47 | 1.4 | (262.64) † | - |
| 5 | 68 | 32 | 1.8 | 227.37 | 0.238 |
| 6 | 85 | 15 | 2.1 | 170.66 | 0.278 |
| 7 | 100 | 0 | 3.4 | 106.87 | 0.34 |

* Approximate layer thickness
† Estimated by interpolation

An example of the resulting microstructures is shown in Figure 1, which is a backscatter scanning electron microscope image illustrating the interface between Layers 5 (32 volume% TiB) and 6 (15 volume% TiB). The excellent bonding of the layers and lack of a distinct interface are apparent in this figure. In addition, the two distinct morphologies of the TiB are shown. The blocky and needle shaped TiB particles (darkest phases) are similar to those previously observed by Tsang, *et al.* [*11*]. A semi-continuous grain boundary network of the NiTi reaction product (lightest phase) from the sintering aid can also be observed in these two layers.

Elastic modulus and Poisson's ratio data were measured by slicing thin beams from the FGM. Specifically, bilayer beams were made from Layers 1 and 2 and from Layers 6 and 7. Trilayer beams were cut from Layers 3, 4 and 5. Longitudinal and transverse strain gages were bonded to one side of each beam. These beams were loaded in four-point bending on one side, then flipped over, re-gaged and again loaded. The modulus and Poisson values calculated from these bending experiments using composite beam theory are listed above (Table 1).

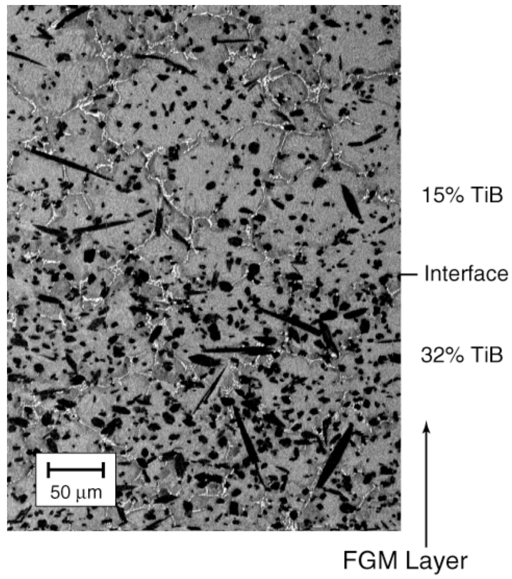


*Figure 1 – Scanning electron microscope image of the layer 5 (32% TiB) and 6 (62% TiB) interface.*

*Residual Stress Measurements*

Residual stresses were measured in the FGM in order to account for their influence on measured toughness. Residual stresses were found in 6.4 mm wide samples removed from the full thickness of the parent FGM plate. The measurements followed the general procedures of the compliance method [*12*], where strains are measured as a slot is incrementally cut through the thickness of the sample. Residual stress normal to the slot is found as a function of slot-depth, computed from the strain versus slot-depth measurements and based on elastic stress release. The calculation scheme employs elastic finite element solutions that account for the variation in material properties present in the FGM.

Slotting proceeded from the TiB-rich side of the FGM. Two strain gages were used, as shown in Figure 2, one located next to the start of the slot, and one opposite this location, but centered on the slot-plane. Coordinates used are also shown in the figure, indicating that $x$ corresponds to the slotting direction. Cutting was performed using electric-discharge machining (EDM) to ensure that as little material was disturbed a possible. Slotting was performed in increments of 0.127 mm (0.005 inch) for the first six increments, and then in increments of 0.508 mm (0.020 inch) for the remainder.

Stresses were computed by representing the unknown residual stress in the Legendre polynomial basis, and using released strain to find coefficients of the basis functions. It was assumed that the variation in material properties in the FGM is sufficiently smooth not to produce large stress discontinuities at the layer interfaces, so that residual stresses can be expressed as a polynomial in the thickness coordinate. For through-thickness residual stress measurements, the constant and linear terms in the polynomial series are not included because they do not satisfy equilibrium. Higher order Legendre polynomial terms do satisfy equilibrium. Using these assumptions, the unknown residual stress, $\sigma_{RS}(x)$, was written as a sum of Legendre polynomial terms, $P_i(x)$, each with a corresponding amplitude, $A_i$

$$\sigma_{RS}(x) = \sum_{i=2,m} A_i P_i(x) \tag{1}$$

In this equation, $m$ represents the order of the highest term in the series. A finite element model was constructed to relate the stress given by a particular basis function, with unit amplitude, to strain release at the location of the strain gages. For a particular basis function, $P_j(x)$, and slot depth, $a_i$, the finite element model was used to find the corresponding strain

$$C_{ij} \equiv \varepsilon(a_i)\big|_{\sigma=P_j(x)} \tag{2}$$

Repeating this analysis for all members of the basis functions and all slot depths resulted in a linear system relating basis function amplitudes to strain as a function of slot depth

$$\varepsilon(a_i) = \sum_{j=2,m} C_{ij} A_j \tag{3}$$

or, using matrix notation

$$\underline{\varepsilon} = \underline{\underline{C}}\,\underline{A}. \tag{4}$$

Given this system, and strains measured experimentally during cutting, the amplitudes of the stress expansion are found by inversion of Equation 4 in a least squares sense

$$\underline{A} = \left(\underline{\underline{C}}^T \underline{\underline{C}}\right)^{-1} \underline{\underline{C}}^T \underline{\varepsilon} \tag{5}$$

Once these amplitudes are found, stress existing in the FGM prior to slotting is obtained from Equation 1.

Finite element calculations were carried out using a commercial finite element package [*13*]. All computations were preformed assuming plane strain. The model had 2620 quadratic (serendipity family) elements and 8163 nodes and exploited the symmetry of the residual stress state about the crack plane, therefore assuming the shear stress on the slotting plane was negligible. The mesh was sufficiently refined that doubling the mesh density in both directions had a negligible effect on the strain versus depth profiles in Equation 2. Material variations were handled by specifying spatially-dependent material constants at the integration points of the elements, as discussed in [*14*]. Strains were computed by differencing nodal displacements at the boundaries of the gage and dividing by the undeformed length, and therefore account for strain gage averaging.

Data reduction and error analysis were performed using available software. Matrix computations were performed using a commercial package [*15*]. Custom software was developed to route the finite element output to the input of the matrix processor. Stresses were computed for several assumed orders of the polynomial series for stress ($m$ in Equation 1). The optimal order of series expansion was selected by plotting the root mean square of the error between measured strain and the fitted strain of Equation 4. Low-order polynomials generally produce high error due to lack of fit, and increasing order

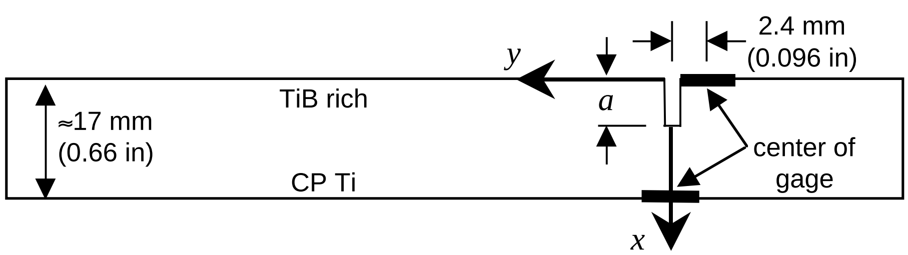


*Figure 2– Typical gage location for slotting.*

decreases error only for a limited number of terms. The numerical condition of the inverted matrix in Equation 5 also becomes poor with increasing number of terms, so that experimental errors can have significant impact on residual stress measurements when an unduly large number of terms are taken in the stress expansion. Therefore, an optimal number of terms must be selected to ensure a good fit to the measured strain while not amplifying experimental errors. In this work, the optimal order of polynomial series was determined by plotting the root mean square error versus order number, and selecting the order at which the error reached a plateau. This has been shown to be a reliable method of selecting the polynomial order in Equation 1 [*16*]. Once the order is selected, error bounds were found for the residual stresses using Monte Carlo. Both slot depth and measured strain were assumed to be normally distributed random variables, with mean equal to the measured value and standard deviation of 0.001 inch for slot-depth and 3 $\mu\varepsilon$ for strain.

The effect of residual stress on measured toughness was found by superposition. Residual stresses were measured in samples of larger dimension those of the SE(B) samples used for fracture testing. Residual stress redistribution resulting from removal of the SE(B) specimen from the larger FGM was found by finite element modeling. The analysis involved distributing an initial stress field, corresponding to the measured residual stress, within a model of the SE(B) geometry, and finding the new equilibrium stress state accounting for the removed material. The contribution of the redistributed residual stress field to the total stress intensity factor during fracture testing was found using a weight function for a homogeneous single edge cracked panel [*17*]. The total stress intensity factor at any point during fracture testing was computed by adding the contributions from residual stress and applied loading. Since the analysis assumes linear elastic behavior, the residual stress correction is valid when the crack-tip is in a brittle region.

### *Fracture Testing*

Fracture testing was conducted using single-edged-notched bend specimens (SE(B)) cut from the FGM using EDM. This material was expected to exhibit rising R-curve behavior during propagation of a crack from the brittle side (containing 85 volume% TiB) toward the ductile titanium layer. For that reason, the specimens were oriented with the machined notch on the side containing the highest concentration of TiB. The machined specimens had a width of 14.73 mm, a thickness of 7.37 mm and a length of 79.50 mm, with a notch 5.08 mm deep (initially $a_o/W = 0.345$) with integral clip gage knife-edges in accordance with ASTM Test Method for Measurement of Fracture Toughness (E1820-96). Prior to fracture testing, one face of each specimen was carefully polished to a mirror finish using diamond and silicon carbide media. The polished surface facilitated measurement of the crack length during crack growth using a traveling microscope. The precracking and fracture experiments were conducted at room temperature on a servohydraulic load frame under computer control. Crack mouth opening displacements were measured using a cantilever type clip gage, as suggested in E1820-96.

It is well-established that fracture toughness testing requires the generation of a short, sharp precrack at the root of the machined notch. Although the procedures appropriate for metals are well-accepted and a number of methods have proven successful for brittle ceramics [*18-21*], there are no established precracking methods for functionally graded materials. In addition to the usual difficulties of controlling the crack length in a relatively brittle material, the varying properties of the FGM present unique challenges in developing a suitable precracking technique.

As a starting point, precracking was attempted using the method described in E 1820-96 by loading the beams in three-point bending under load control. The initial maximum load was 490 N, the load ratio was 0.1 (minimum/maximum load) and the loading span was 63.5 mm. Crack growth was monitored by crack mouth opening displacement (CMOD) compliance. After 75 000 cycles, no change in compliance had been detected, so the maximum load was increased to 540 N. At this load level the crack popped-in to a length of 6.29 mm (a/W = 0.427), as detected by CMOD compliance based on the initial effective modulus. This crack was longer than the desired starting crack length of 5.28 mm (a/W = 0.358) and prevented the fracture toughness testing of two layers in the FGM specimen. Further, a similar approach with another specimen resulted in unstable crack growth to a total length of 14.65 mm (a/W = 0.995). Thus, it was concluded that this method did not provide sufficient control to reliably generate sharp precracks in this relatively brittle material.

Suresh and Brockenbrough have shown that axial compression of ceramic materials leads to precrack initiation by residual tensile stresses during compressive unloading [*18*]. This method was further developed by Ewart and Suresh [*19*]. The layer of the Ti/TiB FGM at the root of the machined notch is brittle, hence it is reasonable to expect that this method of precracking may be effective in functionally graded materials of this type. In order to explore this possibility, SE(B) specimens 50mm in length were machined in the manner described earlier. These shorter specimens and a hemispherical loading fixture were used to prevent buckling and shear failure of the beams in axial compression. A gross stress of 212 MPa was found to be necessary to initiate precracking. This value is only slightly below the yield strength of the CP titanium layer (280 MPa). Short cracks were observed at the root of the machined notch, predominantly oriented in the direction of the loading axis rather than in the desired perpendicular direction. However, the high stress necessary to initiate cracking in the relatively brittle layer also resulted in plastic deformation of the titanium-rich layers. These stresses resulted in microstructural damage (cracking and debonding of the TiB particles from the matrix in the titanium-rich layers) which was observed by scanning electron microscopy. In addition, the average elastic modulus calculated from compliance in three-point bending changed from 145 GPa prior to axial compression loading to 96 GPa after precracking. Due to this microstructural damage, the axial compression technique was deemed unsuitable for use in this study.

Based on limitations of the methods described above, a new precracking method was developed for FGMs and is described in detail in a related paper [*22*]. In order to create compressive stresses at the crack tip and simultaneously avoid tensile deformation in the pure titanium layer, the SE(B) specimens were cyclically loaded in reverse four-point bending, as shown in Figure 3, at a 6 800 N maximum load. The load was applied with a load ratio R = 0.1 at a cyclic frequency of 5Hz. These loading conditions were selected with the goal of developing the precrack in approximately 5 000 cycles. In order to achieve the desired a/W = 0.358 for the fracture experiments, the target precrack length was 0.2 mm. The starting notch and resulting sharp precrack developed by reverse four-point bending fatigue are shown by optical micrographs in Figure 4. The effective

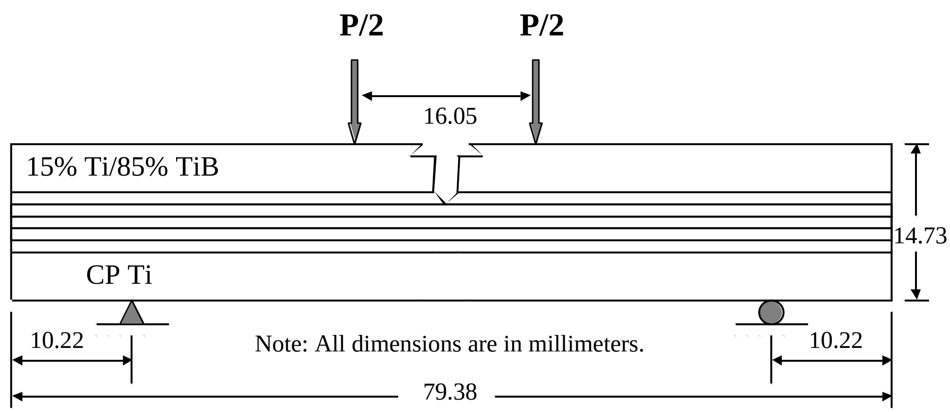


*Figure 3 – Seven-layer Ti/TiB reverse four-point bending specimen.*

*(a)*

*(b)*

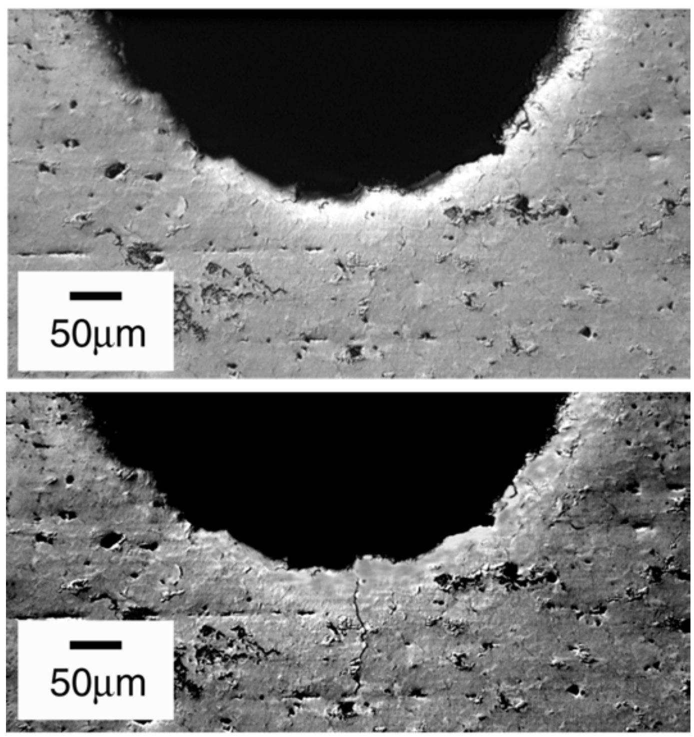


*Figure 4 – (a) EDM notch in Ti/TiB FGM and (b) precrack resulting from reverse four-point bending fatigue.*

modulus was 145 GPa before and after precracking, indicating that, in contrast to the axial compression method, reverse four-point bending did not damage the overall microstructure of the FGM. After precracking, the specimens were heat tinted at 400°C and cooled overnight to room temperature prior to fracture testing.

Fracture tests of the precracked beams were conducted in general accord with the provisions of ASTM E1820-96. The outer loading span for these tests was 58.93 mm (S = 4W). The load on each specimen was initially cycled twenty times at 2 Hz between 22.6 to 184.4 N to seat the clip gage. The load *versus* CMOD compliance of the specimen was determined by loading three times from 89.2 to 266.7 N. The specimen was then loaded to 356.0 N at a rate of 22.26 N/sec, after which the compliance was again measured three times by reducing the applied load by 177.5 N and reloading. Subsequently, the force was increased by the amount necessary to increase the crack mouth opening displacement by 0.0005 mm and the compliance was again measured by the above procedure. After each such increment, the specimens were held for 30 seconds to accommodate any time dependent crack extension. Because the elastic modulus of the FGM varies as the crack extends, the conventional compliance calibration could not be used to determine crack length. Accordingly, independent crack length measurements were taken after each increment of crack extension using a traveling microscope to observe the polished specimen surface.

The fracture tests were continued until the cracks had propagated into the final layer except for two tests that were terminated prematurely to study the mechanisms of crack interaction with the TiB particles in Layers 5 and 6, respectively. After testing, the specimens were removed from the load frame and heat tinted at 400°C in air for 15 minutes and cooled to room temperature. The initial and final cracks were measured in accordance with ASTM E1820-96 using a nine-point average. The initial crack lengths ranged from 5.1 to 5.23 mm (a/W = 0.34 to 0.37). The final crack fronts were straight to within 5% deviation.

## Results

### *Residual Stress Results*

Residual stresses were measured in samples removed from four locations of the FGM plate. Released strain for one particular experiment is shown as a function of slot depth in Figure 5. Error in the strain fit is plotted in Figure 6 versus the highest order of polynomial assumed in the stress expansion, indicating an optimal order of 10 (nine terms in the series). The strain fit resulting from Equation 3 and a $10^{th}$ order polynomial is shown in Figure 5. The residual stress at all four measurement locations is shown in Figure 7, with the optimal order of stress expansion given in the legend for each location. Redistributed residual stress and stress intensity were computed from residual stress measured at location 8-1. Figure 8 shows the original and redistributed residual stress together with the residual stress intensity factor, $K_{RS}$.

These results indicate that the residual stresses have a negative contribution to the crack driving force for crack size a > 2.7mm (a/W ≥ 0.2). Since laboratory fracture measurements are based on measured load, they assume that $K = K_{appl}$. The actual state at the crack tip is more correctly indicated by $K = K_{appl} + K_{RS}$. In the absence of residual stress, one would measure the true material toughness, $K_{material}$. When residual stresses are present, and have been measured, the laboratory measurements, $K_{meas}$, can be corrected by the known $K_{RS}$ using

$$K_{material} \approx K_{meas} + K_{RS}. \tag{6}$$

Therefore, the results shown in Figure 8 indicate that fracture testing, without correction for residual stress, will over-estimate material toughness for a/W > 0.2.

### *Fracture Results*

Fracture toughness was calculated from the load *versus* optically-measured crack

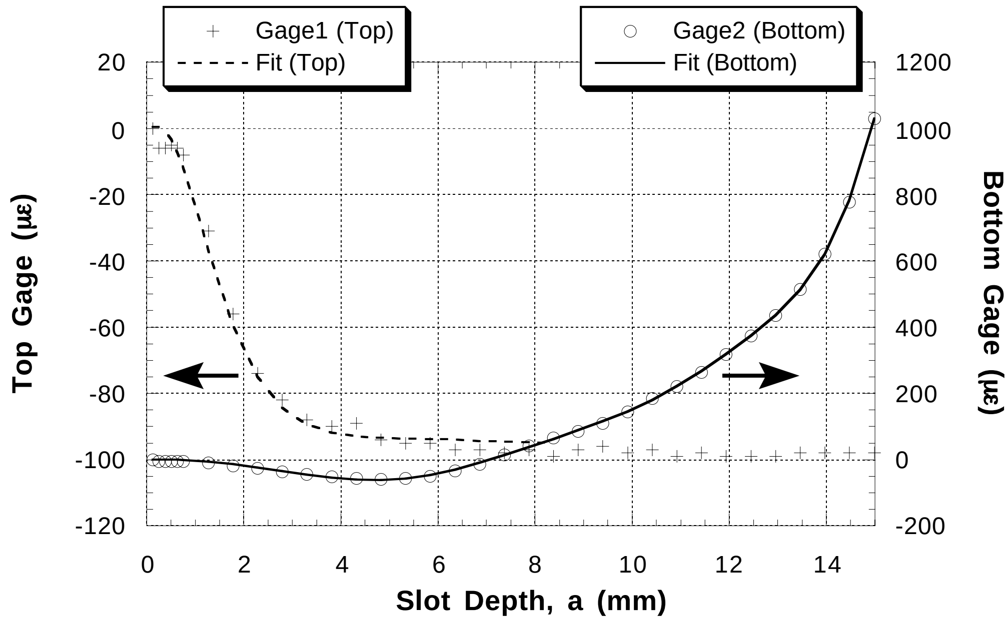


*Figure 5 – Strain release and numerical fit for slotting location 8-1.*

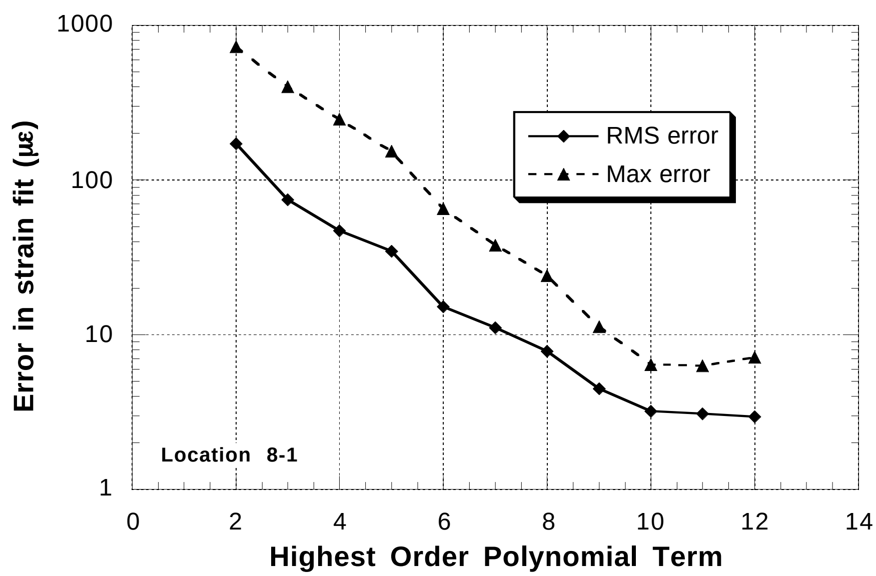


*Figure 6 – RMS and maximum error in strain fit for measurement location 8-1.*

length data using the standard formula for linear elastic, isotropic materials. These measured values are designated $K_{meas}$ because it is not possible to completely verify the validity of the fracture toughness values for this functionally graded material. An example of the results for specimens precracked by the three different methods is illustrated in Figure 9(a). These data reveal rising $K$ behavior as the crack grows into successive layers with increasing metal content. The locations of the interfaces between the layers are noted on the plot.

The beam without a precrack exhibited rapid, unstable crack growth when loads were increased to the point of crack initiation and gave limited useful fracture toughness

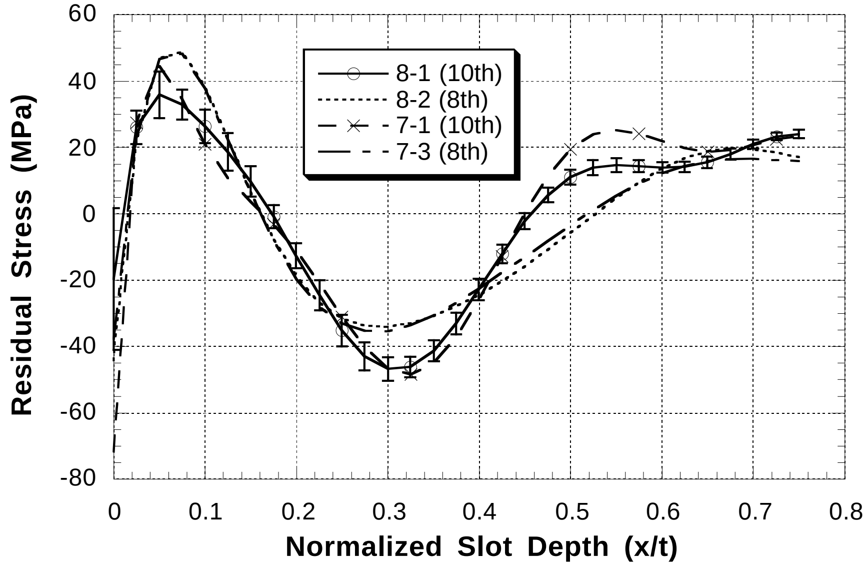


*Figure 7 – Measured residual stress for all four locations. Error bars shown for location 8-1.*

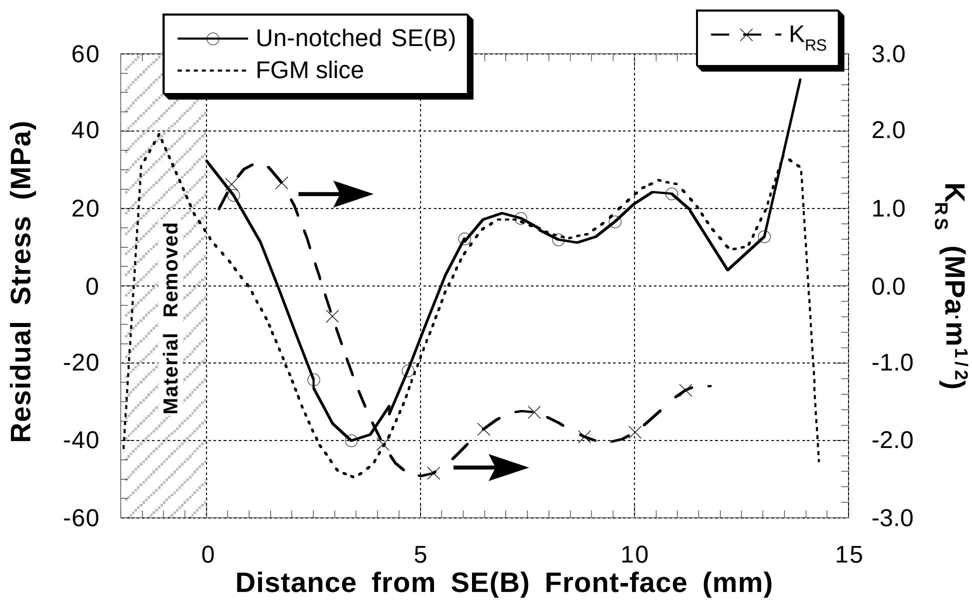


*Figure 8 – Original and redistributed residual stress with $K_{RS}$ for location 8-1.*

data. The specimen precracked by uniform axial compression showed stable crack growth with no pop-in during the fracture test indicating that a sharp crack was initiated during compressive loading. The load values and the resultant *K* values, however, are only 70% of those obtained by the specimen that was precracked by reverse four-point bending. In addition, the initial slope of the load *versus* CMOD curve for this specimen was significantly lower than the slopes of the data for the other two specimens. The lower values for the specimen precracked by axial compression are a consequence of the extensive microcrack damage introduced by this precracking method.

Focussing on the results for the specimen precracked in reverse bending, the present results demonstrate that $K$ rises dramatically, from approximately 7 MPa·m$^{1/2}$ (62% TiB) in Layer 3 to over 30 MPa·m$^{1/2}$ in Layer 6 (15% TiB). This increase in toughness is as expected based on the increasing metal content as the crack propagates toward the Ti rich layer and confirms the general concepts predicted by Jin and Batra [*9*, *10*]. Figure 9(b) illustrates the effect of the residual stresses on the measured $K$ values for the specimen precracked by the reverse four point bending method. Since the residual stresses are negative throughout layers in which the crack propagated, the corrected fracture toughness, $K_{material}$, is less than the nominally measured value, $K_{meas}$. This difference is approximately constant at 2 MPa·m$^{1/2}$ throughout the test.

*(a)*

*(b)*

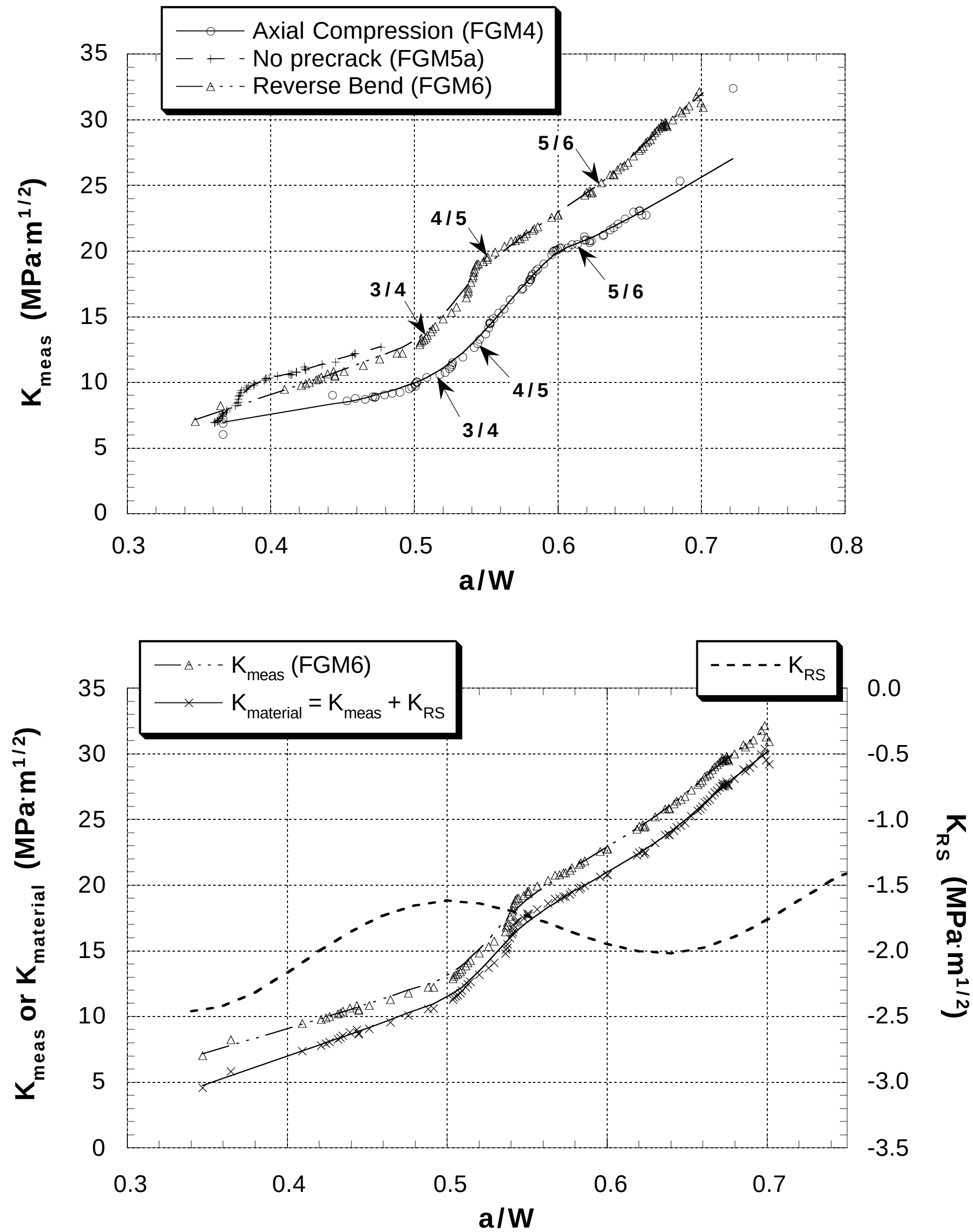


*Figure 9 – (a) Measured $K_I$ R-curves for Ti/TiB FGM specimens precracked by three different methods and (b) measured, residual and resultant material $K_I$ data for fracture test of specimen precracked by reverse four-point bending.*

## Discussion

Accurate measurement of fracture toughness in brittle and ductile materials requires a sharp precrack at the machined notch. In general, the precracking methods that have been developed for homogeneous metallic and ceramic composite materials are not appropriate for FGMs. Since the FGM studied in the present investigation contains both ductile and brittle layers, it was necessary to develop a new method to introduce a sharp precrack in a controlled manner. Conventional fatigue loading such that the notch root experiences tension resulted in unstable crack propagation. Uniform axial compression methods developed for ceramic materials introduced general microstructural damage in the metal-rich layers resulting in lower than expected fracture toughness. In order to combine these loading conditions to subject the notch root to cyclic compression while the metal-rich layers remain in tension, a novel reverse four-point bending method was developed. This new method provided a reliable means by which a controlled, sharp, short precrack was developed at the machined notch in metallic/ceramic FGM beams, allowing accurate fracture toughness measurements. However, it is important to recognize that this method is limited in its applicability to ductile/brittle FGMs. Depending on the properties of the components of a particular FGM, other precracking methods may be more appropriate.

The data for crack propagation in the Ti/TiB functionally graded material clearly reveal rising R-curve results when the crack propagates from the more brittle layers toward the tougher layers. However, the shape of the curve differs substantially from that normally observed in materials that exhibit rising $K_I$ R-curves because of differences in the toughening mechanisms. Although extrinsic toughening mechanisms such as crack bridging and crack deflection are evident in scanning electron microscope images of the crack tip region [*23*], the fracture resistance of the FGM is dominated by increases in intrinsic toughness as the volume fraction of TiB decreases with crack extension. The mechanisms contributing to the intrinsic toughness of the Ti/TiB mixtures include particle cracking and particle/matrix debonding. As the crack propagates through the FGM, however, the volume fraction of Ti increases and these mechanisms become relatively less important.

Because of the significant residual stresses present in the FGM tested in this investigation, the initial measured toughness is significantly higher than the toughness indicated by superposition. This result demonstrates the beneficial effect of the residual stresses in this material. We note, however, that the present results are limited by the fact that the calculated stress intensity values are based on the standard expressions for isotropic, linear elastic solids. Although this approach provides a useful initial estimate and may be warranted in continuously graded materials [*8*], further refinement of this approach is needed for discrete, layered FGMs.[3]

---

[3] Near completion of this manuscript, a weight function for a single edge cracked non-homogeneous plate was published [*24*]. This recent study suggests that for the variation in modulus present in the Ti/TiB FGM, stress intensity factors presented here are reduced by 5-10% relative what would be calculated using the results presented in [*24*].

## Conclusions

The results of fracture testing of a layered Ti/TiB functionally graded material suggest that both the precracking method and residual stresses have a significant effect on the measured toughness. Single edge notch bend (SE(B)) specimens were fabricated so that the crack propagation direction was perpendicular to the graded layers and advancing from the brittle to the ductile side of the FGM. Reverse bending (crack tip in compression) of specimens was found to produce a sharp precrack without damaging the material, and appears to be appropriate for ductile/brittle FGMs. In contrast, uniaxial compression damaged the specimen prior to fracture testing and conventional bending (crack tip in tension) led to unstable and uncontrollable crack propagation.

Rising R-curve behavior for the FGM, starting at $K_{meas}$ = 7 MPa·m$^{1/2}$ in the initial crack-tip location (38% Ti and 62% TiB) was observed in a representative sample. As the proportion of Ti increased with crack advance, toughness increased to $K_{meas}$ = 31 MPa·m$^{1/2}$. Residual stresses acting normal to the crack-plane in the SE(B) specimens were measured in the parent FGM plate using the crack compliance technique. The remaining residual stresses in SE(B) specimens machined from the plate were found computationally, and the weight function was used to determine their influence on fracture toughness. Peak residual stresses were 30 to 50 MPa and for a representative stress profile corresponded to a residual stress intensity factor ($K_{RS}$) of -2.4 MPa·m$^{1/2}$ at the initial precrack length. As a consequence, the actual material toughness at the start of the test was calculated to be $K_{material} = K_{meas} + K_{RS}$ = 4.6 MPa·m$^{1/2}$, or 34% less than that measured by fracture testing. The residual stress intensity factor remained nearly constant with crack extension, hence its relative contribution decreased to approximately 6.5% of the maximum measured toughness.

## Acknowledgments

This paper is based on work supported by the National Science Foundation, Grant CMS 9713798. The authors wish to thank M. B. Prime, W. W. Liang, and E. M. Carrillo-Heian for helpful discussions and Cercom Incorporated for the Ti/TiB FGM material used in this study. The work of W.-Y. Lin for executing many of the residual stress measurements is also acknowledged.

## References

[1] Sasaki, M., Wang, Y., Hirano, T. and Hirai, T., "Design of SiC/C Functionally Gradient Material and its Preparation by Chemical Vapor Deposition," *Journal of the Ceramic Society of Japan*, Vol. 97, 1989, pp. 539-543.

[2] Kawasaki, A. and Watanabe, R., "Powder Metallurgical Fabrication of the Thermal-Stress Relief Type of Functionally Gradient Materials," in *Sintering*, Tokyo, Japan, 1987, Vol. 2, Elsevier, London, pp. 1197-1202.

[3] Fukushima, T., Kuroda, S. and Kitahara, S., "Gradient Coatings Formed by Plasma Twin Torches and Those Properties," in *Proceedings of the First International Symposium, FGM, Sendai*, Tokyo, Japan, 1990, Functionally Gradient Materials Forum and the Society of Non-traditional Technology, pp. 145-150.

[4] Sata, N., Sanada, N., Hirano, T. and Niino, M., "Fabrication of a Functionally Gradient Material by Using a Self-propagating Reaction Process," *Proceedings of the First International Symposium on Combustion and Plasma Synthesis of High-Temperature Materials*, VCH Publishers, Inc., 1990, pp. 195-203.

[5] Miyamoto, Y., Nakanishi, H., Tanaka, I., Okamoto, T. and Yamada, O., "Gas Pressure Combustion Sintering of TiC-Ni FGM," in *Proceedings of the First International Symposium, FGM, Sendai*, Tokyo, 1990, Functionally Gradient Materials Forum and the Society of Non-traditional Technology, pp. 257-262.

[6] Tomasi, A. P., Saiz, E., Ishibashi, H., Diaz, M., Requena, J. and Moya, J. S., "Powder Processing of Mullite/Mo Functionally Graded Materials," *Journal of the European Ceramic Society*, Vol. 18, 1998, pp. 1365-1371.

[7] Erdogan, F. and Wu, B. H., "Analysis of FGM Specimens for Fracture Toughness Testing," *Functionally Gradient Materials, Ceramic Transactions*, American Ceramic Society, Westerville, OH., 1993, pp. 39-46.

[8] Jin, Z.-H. and Noda, N., "Crack-tip Singular Fields in Nonhomogeneous Materials," *Journal of Applied Mechanics*, Vol. 61, No. 3, 1994, pp. 738-740.

[9] Jin, Z. H. and Batra, R. C., "R-curve and Strength Behavior of a Functionally Graded Material," *Materials Science and Engineering A*, Vol. 242, No. 1-2, 1998, pp. 70-76.

[10] Jin, Z. H. and Batra, R. C., "Some Basic Fracture Mechanics Concepts in Functionally Graded Materials," *Journal of the Mechanics and Physics of Solids*, Vol. 44, No. 8, 1996, pp. 1221-1235.

[11] Tsang, H. T., Chao, C. G. and Ma, C. Y., "Effects of Volume Fraction of Reinforcement on Tensile and Creep Properties of in-situ TiB/Ti MMC," *Scripta Materialia*, Vol. 37, No. 9, 1997, pp. 1359-1365.

[12] Prime, M. B., "Residual Stress Measurement by Successive Extension of a Slot: A Literature Review," Technical Report LA-13283-MS, Los Alamos National Laboratory, 1997.

[13] *ABAQUS/Standard*, *Version 5.8*, Hibbitt, Karlsson, and Sorenson, Inc., Providence, RI, 1999.

[14] Giannakopoulos, A. E., Suresh, S., Finot, M. and Olsson, M., "Elastoplastic Analysis of Thermal Cycling: Layered Materials with Compositional Gradients," *Acta Metallurgica et Materialia*, Vol. 43, No. 4, 1995, pp. 1335-1354.

[15] *Matlab, Version 5.3.0*, The MathWorks, Inc., Natick, MA, 1999.

[16] Lin, W.-Y., "Measurement of Residual Stress Distribution Through the Thickness of Functionally Graded Material Ti/$TiB_2$," Master of Science, Mechanical and Aeronautical Engineering Department, University of California, Davis, 1999.

[17] Glinka, G. and Shen, G., "Universal Features of Weight Functions for Cracks in Mode I," *Engineering Fracture Mechanics*, Vol. 40, No. 6, 1991, pp. 1135-1146.

[18] Suresh, S. and Brockenbrough, J. R., "Theory and Experiments of Fracture in Cyclic Compression: Single Phase Ceramics, Transforming Ceramics and Ceramic Composites," *Acta. Metallurgica*, Vol. 36, No. 6, 1988, pp. 1455-1470.

[19] Ewart, L. and Suresh, S., "Dynamic Fatigue Crack Growth in Polycrystalline Alumina under Cyclic Compression," *Journal of Materials Science Letters*, Vol. 5, 1986, pp. 774-778.

[20] *ASTM PS 070-97*, American Society for Testing and Materials, West Conshohocken, PA, 1997.

[21] Sakai, M. and Bradt, R. C., "Fracture Toughness Testing of Brittle Materials," *International Materials Reviews*, Vol. 38, No. 2, 1993, pp. 53-78.

[22] Carpenter, R. D., Paulino, G. H., Munir, Z. A. and Gibeling, J. C., "A Novel Technique to Generate Sharp Cracks in Metallic/Ceramic Functionally Graded Materials By Reverse 4-Point Bending," *Scripta Materialia*, Vol. 43, 2000, pp. 547-552.

[23] Carpenter, R. D., Liang, W. W., Paulino, G. H., Munir, Z. A. and Gibeling, J. C., "Fracture Testing and Analysis of Layered Functionally Graded Ti/TiB in 3-Point Bending," *Acta Materialia*, to be published.

[24] Fett, T., Munz, D. and Yang, Y. Y., "Direct Adjustment Procedure for Weight Functions of Graded Materials," *Fatigue and Fracture of Engineering Materials and Structures*, Vol. 23, No. 3, 2000, pp. 191-198.